Available online at www.sciencedirect.com
ScienceDirect
Carbohydrate Polymers 67 (2007) 97–103
Carbohydrate Polymers
www.elsevier.com/locate/carbpol

Interactions between cellulose and *N*-methylmorpholine-*N*-oxide

Haibo Zhao, Ja Hun Kwak, Yong Wang, James A. Franz, John M. White, Johnathan E. Holladay *

Pacific Northwest National Laboratory, Institute for Interfacial Catalysis, P.O. Box 999, Richland, WA 99352, USA

Received 16 March 2006; accepted 15 April 2006
Available online 9 June 2006

Abstract

Cellulose II structure was obtained when cellulose precipitated from NMMO/H_2O/cellulose solution by adding excess water. The regenerated cellulose was three times more reactive than that of untreated cellulose in hydrolysis reactions. X-ray diffraction (XRD), ^{13}C Solid-State Nuclear Magnetic Resonance (NMR) and Fourier Transform Infrared (FTIR) Spectroscopy were used to investigate interactions between *N*-methylmorpholine-*N*-oxide (NMMO) and cellulose. Cellulose NMMO solid mixtures were heated to various temperatures and cooled to room temperature. The presence of cellulose in cellulose NMMO solid mixture decreased the NMMO melting point by 80–110 °C and hampered NMMO recrystallizing during cooling process. NMMO crystal structure collapsed between 70 and 100 °C in cellulose NMMO mixture and became very mobile (liquid like form). Mobile NMMO molecules transformed crystalline cellulose into amorphous cellulose. When the cellulose NMMO mixture was heated to 150 °C, cellulose started to replace H_2O molecules that hydrogen-bonded to NMMO. Our FTIR spectra results suggest that released H_2O molecules exist as both adsorbed H_2O molecules on cellulose and unbound H_2O molecules that are physically confined in cellulose matrix.

Keywords: Cellulose; *N*-Methylmorpholine-*N*-oxide; NMMO; Hydrolysis; Phase change; Crystallization; XRD; NMR

1. Introduction

Natural cellulose forms unique microcrystal structures through strong hydrogen bonding networks, which greatly limits the access of β-1,4-glycosidic bonds and the other functional groups to reactants and catalysts in heterogeneous reactions. Decrystallization is the most important step to increase cellulose reactivity in heterogeneous reactions. Because cellulose is insoluble in water and most common organic liquids, the utilization of cellulose through modification or depolymerization in homogeneous reactions is also limited. Inventing and employing appropriate solvent systems in homogeneous reactions is a key factor to improve cellulose reactivity.

Cellulose can dissolve in several solvent systems, which include heavy metal-amine complex solutions, concentrated metal salts, cold NaOH solutions, thiocyanate/amine, LiCl/dimethylacetamide (DMAc), *N*-methylmorphine-*N*-oxide (NMMO)/H_2O system, and concentrated H_2SO_4 and H_3PO_4 (Johnson, 1985). The NMMO/H_2O system is the only industrialized solvent for the spinning of cellulosic fiber (Lyocell process) that is used in place of the viscose process (Firgo, Eibl, Kalt, & Meister, 1994). The *N*-methylmorphine-*N*-oxide (NMMO)/H_2O system is able to dissolve up to 30% of high-molecular-weight cellulose (Maia, Peguy, & Perez, 1981) and the dissolution is a physical process without derivatization (Rosenau, Hofinger, Potthast, & Kosma, 2003). However, the processes occurring on the molecular level during dissolution of cellulose in NMMO remain largely unknown. Swelling and dissolution of cellulose will disrupt the hydrogen bonding networks in cellulose by forming new H-bonds between solvents and cellulose. However, these processes are extremely complicated and no individual step has been identified so far. A better understanding of interactions between cellulose and solvent molecules is not

* Corresponding author. Tel.: +1 509 375 2025; fax: +1 509 372 4732.
E-mail address: john.holladay@pnl.gov (J.E. Holladay).

0144-8617/$ - see front matter © 2006 Elsevier Ltd. All rights reserved.
doi:10.1016/j.carbpol.2006.04.019

only important to improve the current Lyocell process, but also to benefit other cellulose utilization processes.

The cellulose regenerated from concentrated $ZnCl_2$ (Chen & Yang, 1985) and CdO/ethylene diamine/H_2O (Tsao, Ladisch, & Ladisch, 1981) systems has shown significantly increased reactivity in hydrolysis reaction. The regenerated cellulose from these solvent systems loses some crystallinity and is closer to an amorphous structure. The cellulose regeneration process from NMMO solvent system may cause phase transition and decrystallization. Learning the structure and reactivity helps the utilization of this regenerated cellulose.

In this paper, we dissolved and regenerated cellulose from a NMMO/H_2O solvent system. The structure of regenerated cellulose was characterized and the reactivity of regenerated cellulose was tested in a hydrolysis reaction. Cellulose and NMMO mixtures, after heating to different temperatures and cooling down back room temperature, were studied by X-ray Diffraction (XRD), Solid ^{13}C Nuclear Magnetic Resonance (NMR), and Fourier Transform Infrared (FTIR) Spectroscopy. The interactions between cellulose and NMMO are discussed.

2. Materials and methods

2.1. Sample preparation

Cellulose (cotton linters, product no. C6663) and NMMO (97%) were purchased from Sigma–Aldrich. Cellulose was dried in a vacuum oven at 105 °C for 48 h before use and NMMO was used as received without further purification. Cellulose/NMMO mixtures (1:1 mass ratio) were milled with an alumina mortar and pestle in a glove box under N_2 protection. In sealed flasks filled with N_2, four samples (1 g mixture) were heated to 70, 100, 125, and 150 °C for 1 h and cooled down back to room temperature. For comparison, one NMMO sample was also heated to 150 °C for 1 h and cooled down back to room temperature. These samples are characterized by XRD, ^{13}C solid-state NMR and FTIR spectroscopy.

Five grams of NMMO/H_2O (11% wt of H_2O) were heated to 100 °C to give a transparent solvent system. Cellulose (0.5 g) was added to this solvent system and mixed at 100 °C until a transparent solution formed. At 100 °C, 50 ml boiling water was added to the solution and stirred by a glass rod. Cellulose that precipitated from the solution was filtered and washed five times by additional boiling water. This regenerated cellulose was characterized by CP/MAS ^{13}C solid-state NMR and tested in an acid hydrolysis reaction after it was dried in a vacuum oven at 105 °C for 48 h. The ball-milled cellulose sample was prepared by ball-milling cellulose for 6 days on an US Stoneware ball mill machine. A ZrO2 ball (mass of 1 kg and diameter of 1 cm) and 30 g of cellulose were loaded into a polypropylene bottle (500 ml). Spinning speed was set at 60 rpm.

2.2. X-ray diffraction method (XRD)

XRD measurements were performed on a Philips PW3040/00 X'Pert MPD system. The diffracted intensity of Cu Kα radiation (wavelength of 0.1542 nm, under a condition of 50 kV and 40 mA) was measured in a 2θ range between 10° and 50°.

2.3. ^{13}C solid-state NMR

Cross polarization/magic angle spinning (CP/MAS) ^{13}C solid-state NMR experiments were performed on a Chemagnetics CMX100 spectrometer operating under a static field strength of 2.3 T (100 mHz ^{1}H) at 25 °C. The contact time for CP was 1 ms with a proton 90° pulse of 5.5 μs and decoupling power of 45 kHz. The MAS speed was 3 kHz. The delay time after the acquisition of the FID signal was 2 s. The chemical shifts were calibrated by using an external hexamethylbenzene standard methyl resonance at 17.3 ppm. On the same instrument, Bloch decay mode (Single Pulse Excitation) was operated with a proton pulse of 5.5 μs and decoupling power of 45 kHz. The MAS speed was 3 kHz. The delay time after the acquisition of the FID signal was 30 s.

2.4. Fourier Transform Infrared (FTIR) Spectroscopy

KBr pellets of samples were prepared by mixing (2–4 mg) NMMO/cellulose mixture with 200–250 mg KBr (spectroscopic grade) with an alumina mortar. The 13 mm diameter pellets were prepared in a standard tool under a pressure of 1360 atm. IR-spectra were recorded using a Nicolet 740 FT-IR spectrometer with a DTGS detector at 4 cm^{-1} resolution. The N_2 gas flow was used as background for each spectrum and 64 scans were taken per sample.

2.5. Reaction tests

Hydrolysis tests were performed on a Symyx heated orbital shaker system (HOSS). Reactants were sealed in vials (fixed on an aluminum plate) and installed into a Symyx reactor. In our experiments, 0.2 g cellulose and 3.0 g of 0.05 M sulfuric acid solution were loaded into a vial. The reactor was pressurized with 100 Psi N_2. Reactors were heated to 150 °C and shaken at 600 RPM. After 40 minutes' reaction, the reactor was quenched in a cold water bath immediately. The products in vials were analyzed by HPLC.

2.6. HPLC analysis of liquid products

Liquid products were analyzed by HPLC using a Bio-Rad Aminex HPX-97H column. A refractive index detector was used in our analysis. The effluent used in our analysis was 0.005 M H_2SO_4.

3. Results

3.1. Regenerated cellulose

Fig. 1 shows relative cellulose conversions to glucose in hydrolysis reactions. The conversion of untreated cellulose, ball-milled cellulose, and regenerated cellulose (cellulose precipitated from NMMO solution) were normalized to that of untreated cellulose. The cellulose conversion of regenerated cellulose almost triples in comparison with that of untreated cellulose. Reprecipitating cellulose from NMMO solution can increase cellulose conversion greater than ball-milling cellulose, which doubles cellulose conversion in comparison with that of untreated cellulose.

Fig. 2 shows CP/MAS ^{13}C solid-state NMR spectra of untreated cellulose, ball-milled cellulose, and regenerated cellulose. Chemical shifts of crystalline cellulose carbons (C1–C6) remain same when cellulose was ball milled for 6 days. Ball-milling only increases the amount of amorphous cellulose which is evident from the increased peak ratio of $C4_{(79–86\ ppm)}/C4_{(86–92\ ppm)}$ and $C6_{(56–63\ ppm)}/C6_{(63–67\ ppm)}$, but the remaining crystalline cellulose maintains the original crystal structure (cellulose I). Regenerated cellulose shows significant chemical shifts from C1–C6 carbons, which indicates that some phase changes occur in the dissolving and precipitating process. The peaks agree very well with those observed from cellulose II structure by Sternberg, Koch, Prieb, and Witter (2003). The assignments of cellulose II carbons are listed in Table 1. The small difference of chemical shifts could be caused by sample source and NMR machine calibration (~1 ppm). The significantly broad peak at 83.8 ppm in Fig. 2 also indicates that a certain amount of amorphous cellulose was also produced in the dissolving and precipitating process.

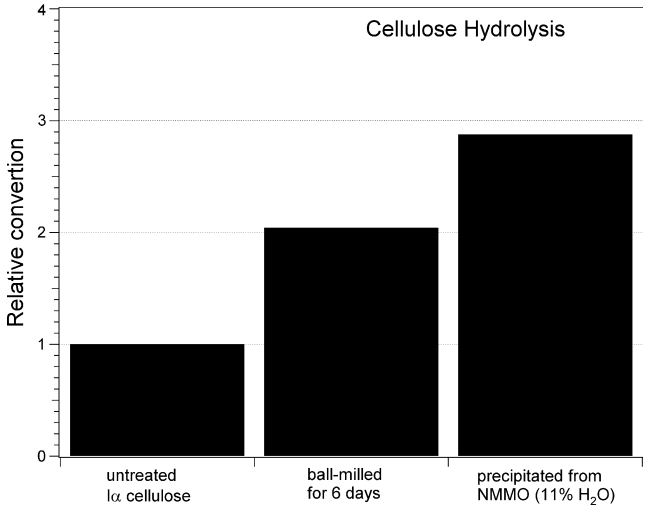

Fig. 1. Normalized cellulose conversion in hydrolysis reaction of untreated cellulose, ball-milled cellulose, and regenerated cellulose.

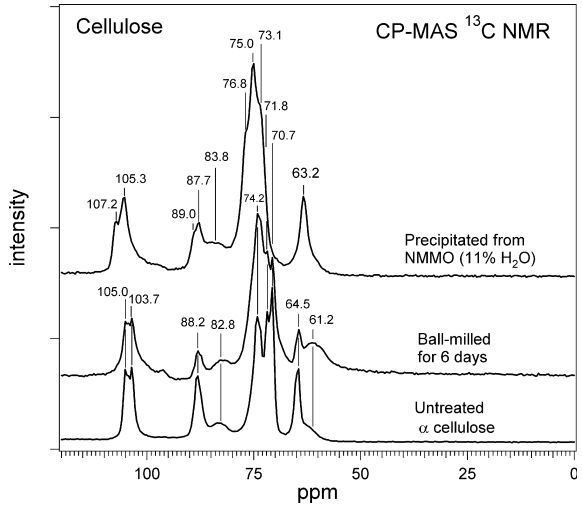

Fig. 2. CP/MAS ^{13}C solid-state NMR spectra of untreated cellulose, ball-milled cellulose, and regenerated cellulose.

Table 1
CP/MAS ^{13}C NMR peak assignments of cellulose II structure

Atom	Chemical shift, ppm (Sternberg et al., 2003)	Chemical shift, ppm (our data)
C1	107.3, 105.4	107.2, 105.3
C2	73.3	73.1
C3	76.9	76.8
C4	89.0, 87.8	89.0, 87.7
C5	75.0	75.0
C6	62.7	63.2

3.2. Cellulose NMMO (1:1 mass ratio) mixture

Fig. 3 shows the XRD patterns of mixture samples that were heated to different temperatures and cooled down to room temperature. The XRD patterns of the untreated NMMO and that was treated at 150 °C are also shown on the inset of Fig. 3. Although some changes occur on the crystalline peaks of NMMO when it was treated at 150 °C, the NMMO crystal structure remains. When the

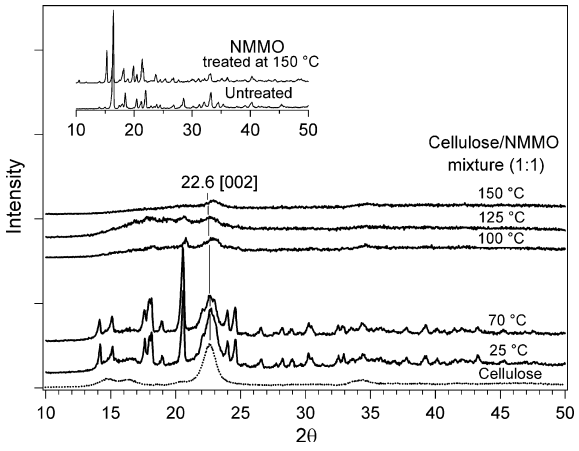

Fig. 3. XRD patterns of cellulose NMMO mixtures that are heated to different temperatures and cooled down. (The XRD patterns of the untreated NMMO and that was treated at 150 °C are shown on the inset.)

mixture was heated to 100 °C and cooled down, most of peaks originating from NMMO crystal disappear and only some strong features between 17° and 21° remain due to residual crystalline NMMO. The strongest cellulose peak, at $2\theta = 22.6°$, originates from the cellulose crystalline plane 002 (Newman, 1999; Park, Kang, & Im, 2004). The intensity of this peak decreased dramatically when the mixture sample was heated to 100 °C and cooled down. When the mixture was heated to 150 °C and cooled down, all crystalline NMMO peaks are gone and the intensity of cellulose crystalline peak reaches the minimum.

Fig. 4 shows the CP/MAS ^{13}C NMR spectra of mixture samples that were heated to different temperatures and cooled down to room temperature. The NMR spectra of the untreated NMMO and that was treated at 150 °C are also shown on the inset of Fig. 4. No significant change was observed on the NMR spectra when the NMMO was treated at 150 °C. The peak at 61.7 ppm originates from crystalline NMMO. The intensity of this peak decreased dramatically when the mixture was heated to 100 °C and cooled down. Further increasing the temperature further decreases the intensity of this peak until it becomes very weak at 150 °C. No chemical shift corresponding cellulose carbon atoms was observed during this heating and cooling process. All the crystalline cellulose remains I structure and no cellulose II structure is produced in this process. When the mixture was heated to 100 °C and cooled down, the peak ratio of $C4_{(79–86\ ppm)}$/$C4_{(86–92\ ppm)}$ increased and suggested that some amorphous cellulose was produced in the process. The peak ratio of $C4_{(79–86\ ppm)}$/$C4_{(86–92\ ppm)}$ reaches the maximum when the mixture was heated to 125 °C and cooled down.

Fig. 5 shows the CP/MAS and Bloch decay ^{13}C NMR spectra of the mixture sample that was heated to 150 °C and cooled down to room temperature. The NMMO signal at 60.4 ppm that almost disappeared in the CP/MAS mode was recovered in the Bloch decay mode. The cellulose C1, C2, C3, and C5 peak signals resolutions in the Bloch decay mode are weaker than those in the CP/MAS mode because of poorer signal to noise ratio in the Bloch decay mode. Partial overlap between the cellulose C6 peak and the NMMO peak makes it difficult to observe changes in the C6 peak. Significant differences are observed in the C4 peak between the CP/MAS and Bloch decay mode. The strong C4 peak of crystalline cellulose between 86 and 92 ppm disappears in the Bloch decay mode.

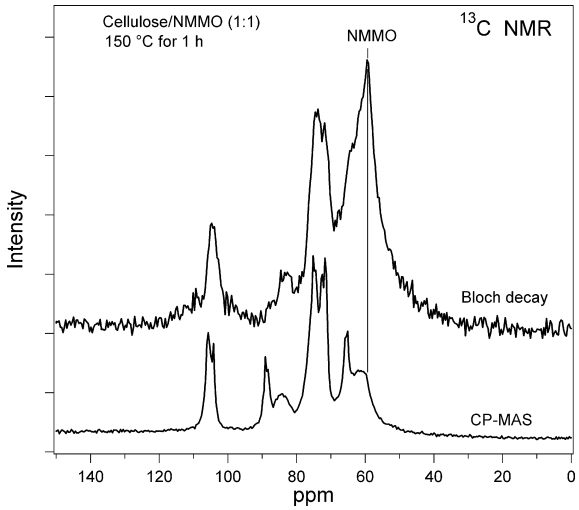

Fig. 5. CP/MAS and Bloch decay ^{13}C solid-state NMR spectra of the cellulose NMMO mixture that is heated to 150 °C and cooled down.

Fig. 6 shows the FTIR spectra of mixture samples that were heated to different temperature and cooled down to room temperature. The spectra between 900 and 1900 cm^{-1} are shown in Fig. 6 because no changes are observed at 1900–4000 cm^{-1} and 600–900 cm^{-1}. The FTIR spectrum of the mixture at 25 °C was the simple summation of pure cellulose and NMMO spectrum. The features of NMMO and cellulose in this mixture did not change

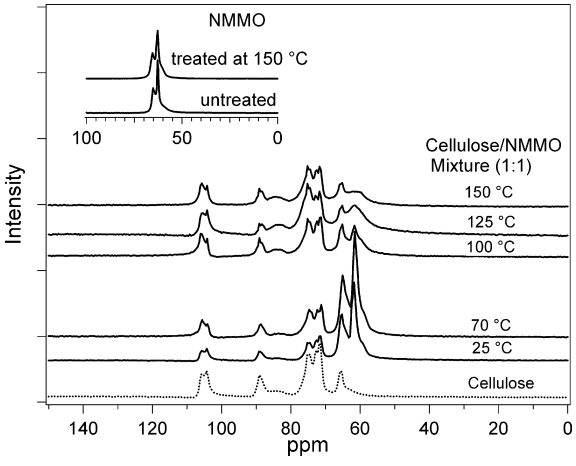

Fig. 4. CP/MAS ^{13}C solid-state NMR spectra of cellulose NMMO mixtures that are heated to different temperatures and cooled down. (The CP/MAS ^{13}C NMR spectra of the untreated NMMO and that was treated at 150 °C are shown on the inset.)

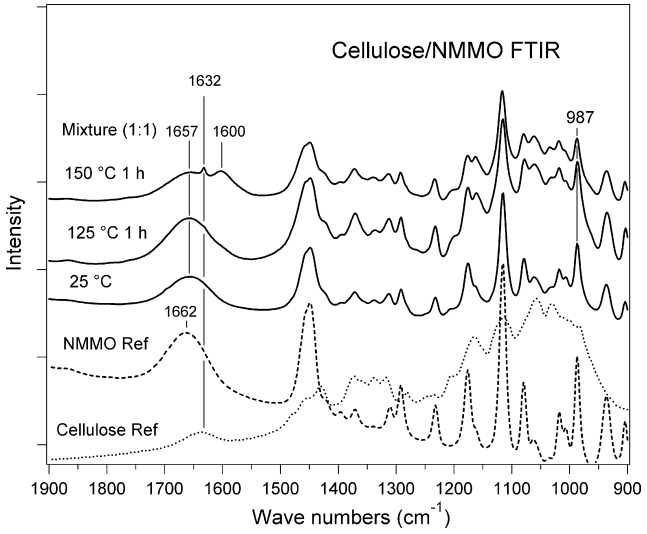

Fig. 6. FTIR spectra of cellulose NMMO mixtures that are heated to different temperatures and cooled down.

when the mixture was heated to various temperatures up to 150 °C. Significant changes occur between 1500 and 1700 cm^{-1}. New peaks at 1632 and 1600 cm^{-1} were observed when the mixture sample was heated to 150 °C and cooled down to room temperature. The peaks at 1657, 1632, and 1600 cm^{-1} are assigned to different water molecules in the mixture. (See Section 4)

4. Discussion

4.1. Regenerated cellulose

If cellulose is dissolved and precipitated, or treated with a concentrated alkaline swelling agent and washed with water (mercerization), cellulose II is formed (French, 1985). All regenerated celluloses have a much lower degree of crystallinity (e.g., ~40%) than the native form (Dudley et al., 1983). Our NMR results show that the dissolving and precipitating process converts cellulose I to cellulose II and amorphous cellulose. Similar structures were previously observed by X-ray diffraction method after cellulose precipitated from NMMO/H_2O/cellulose solution after adding water (Biganska, Navard, & Bedue, 2002). Although more amorphous cellulose is present in the ball-milled sample, the cellulose conversion of regenerated sample is higher than that of ball-milled sample. This fact means that reprecipitating cellulose from NMMO solutions makes more β-1,4-glycosidic bonds accessible to acid catalysts than ball-milling does. The increase of cellulose conversion in hydrolysis after being ball-milled was only due to the increased amorphous part. Our results strongly indicate that cellulose II structure is more reactive (accessible) than cellulose I structure. Due to this reason, reprecipitating cellulose (cellulose II structure) with less amorphous cellulose can be more reactive in hydrolysis than ball-milled sample (cellulose I crystal structure) with more amorphous cellulose.

4.2. Cellulose NMMO 1:1 mixture

The melting point of anhydrous NMMO is found to be 184 °C (Chanzy, Nawrot, Peguy, & Smith, 1982; Navard & Haudin, 1981). The XRD and CP/MAS ^{13}C NMR spectra of the untreated NMMO and that was treated at 150 °C suggest that the NMMO crystal structure was maintained even after NMMO was treated at 150 °C. XRD and CP/MAS ^{13}C NMR spectra of cellulose and NMMO mixtures demonstrated that NMMO crystal disappears and melts even below 100 °C. This fact indicates that the presence of cellulose decreases the melting point of NMMO at least by 80 °C. It is well known that adding 13% of H_2O into NMMO can decrease the melting point of NMMO to less than 76 °C (Chanzy et al., 1982; Navard & Haudin, 1981). The N—O bond in NMMO has a very strong dipole moment and the O in the N—O bond can form one or two hydrogen bonds with hydroxylated substances, such as water and alcohol (Chanzy, Maia, & Perez, 1982; Maia et al., 1981; Maia & Perez, 1982). For example, NMMO and H_2O can form very strong N—O ⋯ H—O—H hydrogen bonds with strengths of 12.01 kcal mol^{-1} in the monohydrate and 15.83 kcal mol^{-1} in the 2.5 mole hydrate (Harmon, Akin, Keefer, & Snider, 1992). Similar hydrogen bonds are also believed to form with cellulose, (Chanzy et al., 1982) which lead to the decrease of the NMMO melting point.

After the cellulose NMMO mixture sample was heated to 100 °C or higher, NMMO does not recrystallize during the cooling process. These NMMO molecules are present in a mobile form or highly dispersed in cellulose matrix. The NMMO molecules are not detected by XRD and CP/MAS ^{13}C NMR spectra. In our XRD and CP/MAS ^{13}C NMR spectra of the mixture samples that were heated to more than 100 °C, only very small amounts of residue crystalline NMMO were detected. The CP/MAS ^{13}C spectroscopy can not detect rapidly reorienting molecules or functional groups undergoing rapid rotation (Komorowski, 1986). Bloch decay ^{13}C NMR detects all resonances provided that sufficiently long recycle delays are employed. In our experiments, 30 s pulse delays were employed because no significant NMMO signal change was observed on changing pulse delays from 30 to 60 s. The missing NMMO signals from mobile NMMO molecules are clearly observed in the Bloch decay ^{13}C NMR, as shown in Fig. 5. The presence of cellulose evidently severely hampers the nucleation and growth of the NMMO crystal at high cellulose concentration. Chanzy et al. reported similar phenomena and thought that polymeric "impurity" can impede the nucleation and growth of crystals because of a retarded diffusion of the crystallization species and poisoning of crystal facets (Chanzy et al., 1982). However, Biganska et al. observed the crystallizing of solvent molecules in an X-ray scattering method when 3% cellulose solution in NMMO/H_2O (15% wt of H_2O) was cooled down (Biganska et al., 2002). They also found that the crystallized pattern disappeared when cellulose concentration increased to 6%. These facts suggest that there is a minimum polymeric "impurity" requirement to prevent solvent molecules to crystallize. In our experiments, cellulose should be more than enough to saturate NMMO and prevents NMMO from crystallizing during the cooling process.

Fig. 3 shows that cellulose crystal structure does not change when NMMO exists in a crystal form below 70 °C. When NMMO crystal structure disappears at 100 °C, it also destroys some cellulose crystal structure in the mixture. The small cellulose crystalline peaks at 100 °C or higher in Fig. 3 originate from residual crystalline cellulose due to excess cellulose in the mixture. The residual crystalline cellulose also accounts for carbon signals of cellulose I in Fig. 4. These results strongly suggest that cellulose does not crystallize when cellulose NMMO solution solidifies during cooling down process although cellulose crystallization in NMMO solution could readily be induced by adding water. Amorphous cellulose struc-

tures were obtained when cellulose solution in NMMO/H_2O (15% wt of H_2O) solidified after cooling down to room temperature (Biganska et al., 2002; Chanzy et al., 1982). Consistent with these findings, the peaks originated from amorphous structure (C4 86–79 ppm) in Fig. 4 are intensified when mixture samples were heated to more than 100 °C. The C4 peak (92–86 ppm) of crystalline cellulose is stronger than that of amorphous cellulose (86–79 ppm), but it disappears in the Bloch decay mode in Fig. 5. Same results are also observed for untreated cellulose in the Bloch decay mode with pulse delay at 30 s. These results suggest that the C4 of crystalline cellulose has a longer relaxation time. When the pulse delay was increased to 60 s, the C4 peak of crystalline cellulose in untreated cellulose was recovered in the Bloch decay mode (spectrum was not shown). These facts indicate that the C4 relaxation time of crystalline cellulose (T1) is between 30 and 60 s.

It is generally thought that strong H-bonds form between cellulosic hydroxyl groups and the N—O group of the NMMO. Surprisingly, no significant peak shifts were observed in Fig. 6 when cellulose and NMMO mixture samples are heated to different temperatures and cooled down. In particular, the ν_s N—O mode at 987 cm^{-1} does not shift when temperature increased from 25 to 150 °C. This indicates that forming H-bonds with cellulosic hydroxyl groups almost has no effects on the ν_s N—O vibration mode. Unlike NMMO and cellulose molecules, the water bending mode ν_{bend} H_2O changes significantly when the temperature is increased from 25 to 150 °C. Below 125 °C, only ν_{bend} H_2O at 1657 cm^{-1} was observed, which was assigned to H_2O molecules bonded to NMMO. The ν_{bend} H_2O at 1632 cm^{-1} was assigned to H_2O bonded to cellulose (Schwanninger, Rodrigues, Pereira, & Hinterstoisser, 2004). The peak at 1600 cm^{-1} is very close to ν_{bend} H_2O of water vapor at 1595 cm^{-1} (Darling & Dennison, 1940). The ν_{bend} H_2O increases by increasing hydrogen bonding and causes ν_{bend} H_2O shift to 1645 cm^{-1} in liquid water (Devlin, Sadlej, & Buch, 2001). The assignments of these peaks are summarized in Table 2. The peak at 1600 cm^{-1} must be from H_2O molecules with almost no hydrogen bond. The source of these H_2O molecules could be explained by the following reason. At 150 °C, cellulose molecules compete with H_2O molecules that are bonded to NMMO. Some H_2O molecules are replaced by cellulose molecules. Some of these released H_2O molecules H-bond to cellulose with ν_{bend} H_2O at 1632 cm^{-1}. The other part of released H_2O molecules are physically confined in cellulose matrix and form no or very weak hydrogen bonds with cellulose. The ν_{bend} H_2O numbers in Table 2 also suggest that the hydrogen bond strengths between these molecules are NMMO—H_2O > H_2O—H_2O > H_2O—cellulose.

Table 2
FTIR spectra peak assignments of ν_{bend} H_2O

ν_{bend} H_2O (cm^{-1})			
Our data		Reference	
H_2O—NMMO	1662	NMMO · 2.5H_2O Harmon et al. (1992)	1660
H_2O—NMMO cellulose mixture	1657	NMMO · H_2O Harmon et al. (1992)	1660
H_2O—cellulose	1632	H_2O—cellulose Schwanninger et al. (2004)	1635
H_2O trapped in cellulose matrix	1600	H_2O (liquid) Devlin et al. (2001)	1645
		H_2O (vapor) Darling and Dennison (1940)	1595

5. Conclusions

Cellulose dissolved in NMMO/H_2O (11% wt of H_2O) solvents at 100 °C and precipitated as a Cellulose II structure after excess water was added to the solution. The conversion of regenerated cellulose in hydrolysis reaction is three times as that of untreated cellulose. Although CP/MAS ^{13}C NMR spectra show that more amorphous cellulose are present in the ball-milled cellulose than in the regenerated cellulose, the activity of ball-milled cellulose is lower than that of regenerated cellulose. These results indicate that cellulose II structure is more reactive (accessible) than cellulose I.

The presence of cellulose in cellulose/NMMO mixture greatly decreased the melting point of NMMO by 80–110 °C and hampered the recrystallization of NMMO during cooling. NMMO crystal structure crashed between 70 and 100 °C. Bloch decay (Single Pulse Excitation) instead of CP/MAS mode must be used to detect these highly mobile NMMO molecules. Cellulose I crystal structure is destroyed and becomes amorphous structure when NMMO molecules become mobile below 100 °C. When cellulose and NMMO mixture was heated to 150 °C, cellulose started to replace H_2O molecules that bonded to NMMO. Our FTIR results suggest that the released H_2O molecules exist as both adsorbed H_2O on the cellulose and unbound H_2O molecules that are physically confined in cellulose matrix.

Acknowledgements

The authors thank Dr. James F. White and Dr. Thomas H. Peterson for helpful and informative discussions. This work was supported by the Laboratory Directed Research and Development Program at the Pacific Northwest National Laboratory (PNNL), a multiprogram national laboratory operated by Battelle for the U.S. Department of Energy under Contract DE-AC06-76RL01830. Part of the research described in this paper was performed at the Environmental Molecular Science Laboratory, a national scientific user facility located at PNNL.

References

Biganska, O., Navard, P., & Bedue, O. (2002). Crystallisation of cellulose/*N*-methylmorpholine-*N*-oxide hydrate solutions. *Polymer, 43*, 6139–6145.

Chanzy, H., Maia, E., & Perez, S. (1982). Cellulose organic solvents. III. The structure of the *N*-methylmorpholine-*N*-oxide-trans-1,2-cyclohexanediol complex. *Acta Crystallographica, B38*, 852–855.

Chanzy, H., Nawrot, S., Peguy, A., & Smith, P. (1982). Phase behavior of the quasiternary system *N*-methylmorpholine-*N*-oxide, water, and cellulose. *Journal of Polymer Science: Polymer Physics Edition, 20*, 1909–1924.

Chen, L. F., & Yang, C. M. (1985) Selective hydrolysis of cellulose to glucose without degradation of glucose using zinc chloride. U.S. patent 4 525 218.

Darling, B. T., & Dennison, D. M. (1940). The water vapor molecule. *Physical Review, 57*, 128–139.

Devlin, J. P., Sadlej, J., & Buch, V. (2001). Infrared spectra of large H_2O clusters: new understanding of the elusive bending mode of ice. *Journal of Physical Chemistry A, 105*, 974–983.

Dudley, R. L., Fyfe, C. A., Stephenson, P. J., Deslandes, Y., Hamper, G. K., & Marchessault, R. H. (1983). High-resolution carbon-13 CP/MAS NMR spectra of solid cellulose oligomers and the structure of cellulose II. *Journal of the American Chemical Society, 105*, 2469–2472.

Firgo, H., Eibl, M., Kalt, W., & Meister, G. (1994). Critical questions on the future of NMMO technology. *Lenzinger Berichte, 74*, 80–90.

French, A. D. (1985). Physical and theoretical methods for determining the supramolecular structure of cellulose. In T. P. Nevell & S. H. Zeronian (Eds.), *Cellulose chemistry and its applications* (pp. 84–111). Chichester, England: Ellis Horwood.

Harmon, K. M., Akin, A. C., Keefer, P. K., & Snider, B. L. (1992). Hydrogen bonding Part 45. Thermodynamic and IR study of the hydrates of *N*-methylmorpholine oxide and quinuclidine oxide. Effect of hydrate stoichiometry on strength of H—O—H ··· O—N hydrogen bonds; implications for the dissolution of cellulose in amine oxide solvents. *Journal of Molecular Structure, 269*, 109–121.

Johnson, D. C. (1985). Solvents for cellulose. In T. P. Nevell & S. H. Zeronian (Eds.), *Cellulose chemistry and its applications* (pp. 181–201). Chichester, England: Ellis Horwood.

Komorowski, R. A. (1986) In High Resolution NMR Spectroscopy of Synthetic Polymers in Bulk (p. 42). Deerfield Beach, FL: VCH.

Maia, B. E., Peguy, A., & Perez, S. (1981). Cellulose organic solvents. I. The structures of anhydrous *N*-methylmorpholine *N*-oxide and *N*-methylmorpholine *N*-oxide monohydrate. *Acta Crystallographica B, 37*, 1858–1862.

Maia, E., & Perez, S. (1982). Cellulose organic solvents. II. The structure of *N*-methylmorpholine *N*-oxide $2.5H_2O$. *Acta Crystallographica, B38*, 849–852.

Navard, P., & Haudin, J. M. (1981). Etude thermique de la *N*-methylmorpholine *N*-oxyde et de sa complexation avec l'eau. *Journal of Thermal Analysis and Calorimetry, 22*, 107–118.

Newman, R. H. (1999). Estimation of the lateral dimensions of cellulose crystallites using ^{13}C NMR signal strengths. *Solid State Nuclear Magnetic Resonance, 15*, 21–29.

Park, C. H., Kang, Y. K., & Im, S. S. (2004). Biodegradability of cellulose fabrics. *Journal of Applied Polymer Science, 94*, 248–253.

Rosenau, T., Hofinger, A., Potthast, A., & Kosma, P. (2003). On the conformation of the cellulose solvent *N*-methylmorpholine-*N*-oxide (NMMO) in solution. *Polymer, 44*, 6153–6158.

Schwanninger, M., Rodrigues, J. C., Pereira, H., & Hinterstoisser, B. (2004). Effects of short-time vibratory ball milling on the shape of FT-IR spectra of wood and cellulose. *Vibrational Spectroscopy, 36*, 23–40.

Sternberg, U., Koch, F. T., Prieb, W., & Witter, R. (2003). Crystal structure refinements of cellulose polymorphs using solid state ^{13}C Chemical Shifts. *Cellulose, 10*, 189–199.

Tsao, G. T., Ladisch, M. R., & Ladisch, C. M. (1981) Process for treating cellulosic materials and obtaining glucose therefrom. U.S. Patent 4 281 063.